Transmittal letter

Professor Matthew Oliver

University of California, Davis

Davis, CA 95616

Dear Professor Oliver:

Enclosed is our completed drone delivery system report. This report is a continuation of our proposal in accordance to the guidelines and sample report provided.

Our report revolves around implementation of practical drone delivery services. Our report addresses critical drone delivery problems keeping planned systems in the prototype stages, such as Amazon's Prime Air.

We look forward to sharing our recommendation report with you. Thank you for your feedback and cooperation.

Sincerely,

Drone Delivery System Division

Enclosures

Drone Delivery System

University of California, Davis

Grammar Squad

January 2018

Table of Contents

Executive Summary iii
Abstract iv
1.0 Introduction 1
2.0 Technical Background 2
2.1 Drone Selection and Deployment 2
2.1.1 The State of Drone Delivery 2
2.1.2 Design Scope Consideration 3
2.1.2 Multicopter Designs 4
2.1.3 Fixed Wing Design 6
2.1.4 Deployment Considerations 7
2.1.5 Conclusion 8
2.2 Battery 9
2.2.1 Charging Schedule 9
2.2.2 Adaptive H Infinity for Charging Schedule 10
2.2.3 Battery Assignment 11
2.2.4 All Climate Battery for Low Temperature 13
2.2.5 Conclusion 16
2.3 Routing Algorithm 16
2.3.1 General Idea of Routing Algorithm 16
2.3.2 Flow Network Model 17
2.3.3 Optimization Problem in Rural and Exurban Areas 18
2.3.4 Optimization Problem in Urban Areas 23
2.3.5 Final Solutions 25
2.3.6 Conclusion 26
2.4 Cyber Security
2.4.1 Ground Station 26
2.4.2 XBee 868LP Chip 28
2.4.3 Wifi Link 29
2.4.4 Telemetry Link: MAVLink Protocol 30
2.4.5 Microcontroller 31
2.4.6 Electroencephalogram (EEG) signal 32
2.4.7 Encryption 33
2.4.8 Conclusion 34
3.0 Criteria and Comparison Strategies 35
3.1 Drone Design and Deployment Comparison 35
3.2 Battery Comparison 38
3.3 Routing Algorithm Comparison 39
3.4 Security Feature Comparison 40
3.5 Cyber Security 41
4.0 Recommendation 43
5.0 Conclusion 44
6.0 References 46
7.0 Division of Responsibilities 49

Executive Summary

Several large companies have suggested using drones for delivery, but all proposed systems are in testing. Ongoing testing by Amazon, Google, etc. have not guaranteed the security, efficiency, and profitability of drone delivery system in the US. After researching the situation, our group has found improvements that can be applied to many of the prototype drone delivery systems.

By using modular multicopters with removable batteries, the cost of maintaining a drone fleet is reduced, and modifying current delivery vehicles will allow for easy deployment to address the last miles. Battery replacement and charging costs can be minimized by creating a charging schedule. A charging schedule can be used to assign the lightest possible battery per flight path in addition to reducing overall charging time. This will result in a quicker delivery system and improved battery lifetime for delivery drones. The drones can find the most efficient routes possible through mathematical models that determine their flight patterns. Intruders can be prevented from hacking and stealing the drones by removing common backdoors.

Further research into all-climate batteries, which are still in prototyping, is needed. There are fixed wing craft that might become better than multicopters in the future. Interaction with other drone depots has not been accounted for, as drones begin and end their flight in trucks. Cybersecurity is an ongoing battle in any field.

Despite these hurdles, our research and the work of large entities such as Amazon and Google reinforces the feasibility and cost-effectiveness of our Drone Delivery System.

Abstract

This paper proposes a drone delivery system which accounts for drone design, battery choice, flight routes, and cybersecurity. Although drone delivery gained attention in 2013 with the announcement of Prime Air, no such system is publicly available yet. The strategy for a drone delivery system uses trucks to deploy drones for the last miles, utilizing the drones' flight capability to reduce travel time and distance. However, experts recognize typical flight time as a weakness in the system. Drone delivery is hindered from limited battery life and costly battery replacement. Battery lifetime can be improved by lighter weight batteries and charging schedules. Mathematical models can optimize drone flight paths. Current security flaws allow crashing of the control system in a drone or hijacking. Encryption and addition of functionalities to the communication protocols may patch the shortcomings of the security protocol. The sum of these solutions is a strong drone delivery system.

1.0 Introduction

Amazon famously announced their plans for a drone-based delivery service in 2013, but such services are not available in the US despite interest from other large companies such as DHL, UPS, and Google [1], indicating issues with the available technology. The typical drone, or unmanned aerial vehicle (UAV), can stay in the air for 30 minutes, but that decreases appreciably when loaded, and requires an hour before its battery is fully recharged [2]. When examining battery life for multirotor drones, results show that energy consumption varies linearly with payload weight and battery [1]. The lack of a secure communication link between drone and ground station pose a safety hazard for individuals hindering deployment of drones as delivery vehicles. A drone delivery system is constructed based on flow network to optimize energy consumption and delivery efficiency.

This project aims to identify and optimize the aspects of a drone delivery system. Among these aspects are the drone itself, the battery selected, the flight paths, and protection against cyber-attackers. Summarily, the aim is to develop drone deliveries beyond the scarce bits shown by prospective delivery companies such as Amazon.

2.0 Technical Background

2.1 Drone Selection and Deployment

2.1.1 The State of Drone Delivery

Several large entities such as Amazon, Google [1], and UPS [3] have expressed interest in drone delivery. However, no such service is available in the United States as of 2018, despite testing by each company [3][4][5]. Trouble with US airspace regulations is often cited as the cause of this delay, hence the amount of testing in other nations, and Amazon has created several proposals regarding airspace access for small drones [4]. Each company continues to develop new designs for their drones, though, and even Amazon is still ideating how to handle supporting infrastructure for the drones [6].

2.1.2 Design Scope Consideration

Increased flight time is always a desired outcome except when stability is required for environmental conditions or extra carrying capacity is necessary. Operation in cramped urban environments is certain, thus any drone selected should be capable of vertical take-off and landing (VTOL) and should be much smaller than traditional aircraft. Batteries must be removable, as average flight time for a drone is 30 minutes and can take an hour to recharge fully [2]. In fact, the drone should be as modular as possible. Parts commonality will dictate all motors used are the same. Finally, although Amazon considered parachute-dropping their packages [6],

this method of package-drone separation will not be covered due to the obvious risks to package integrity.

2.1.3 Multicopter Designs

The multicopter (MC) is the iconic drone design and easily recognizable by the multiple motors adorning its frames. The most common MC's are quadcopters (4 rotors), hexacopters (6 rotors), and octocopters (8 rotors). Any other design must be compared to the MC's due to their sheer prevalence. Most of the companies exploring drone delivery use these types of drones. Consider this section a review of drone basics.

Environmental conditions and purpose should be considered when choosing the number of motors a drone should have:

> "The number of motors and configuration of each type of multicopters has an influence on their performance. For instance, the more motors a multicopter has, the more power it has for its take-off (more lift capacity) and it can then carry more payloads. However, increasing the number of motors will affect the power consumption, hence bigger batteries are required to gain more flight time. Besides that, each time a DC brushless motor is added to a multicopter, an additional Electronic Speed Controller (ESC) is required to control it" [7].

Zulkipli et al. created a reference table (Table 1) for various MC configurations with a given motor to illustrate these principles.

Table 1: Minimum throttle inputs for various configurations. For takeoff, a motor must produce twice the weight of the drone (and package) in lift [7].

Parameters	Tri-copter	Quad-copter	Hexa-copter	Octo-copter
Take-off weight (g)	900	1000	1200	1600
Number of motors	3	4	6	8
lift per motor (g)	300	250	200	200
Min throttle(%) for take off	45-50	40	30-35	30-35

Flight time of a single motor decays exponentially as throttle increases (Figure 1), and electrical component lifespan will also decrease, and the heat produced at higher throttles indicates reduced efficiencies [7].

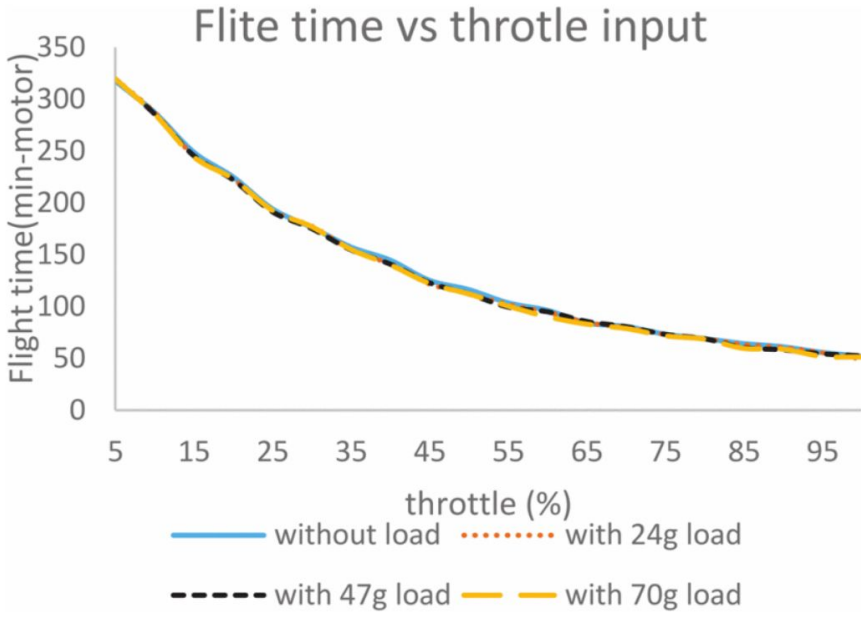

Figure 1: Flight time (min * motor) vs. throttle [7].

Approximating from Figure 1, for 4, 6, and 8 motors, this means flight times of 38, 30, and 21 minutes, respectively. It should be noted that the motors used all had the same propellers which, based on length and number of blades, can greatly affect the efficiency of motor. Stopforth et al. detailed their experiments with propellers regarding efficiency for their dual motor drone and discovered complicated relationships with the RPM of their chosen motor [8].

The quadcopter's flight time makes it a promising choice, but environmental factors may render it a nonoptimal choice for some regions and weather. Abarca et al discuss the advantages of a hexacopter over a quadcopter when dealing with extreme weather at high altitudes:

> "A hexacopter setup was chosen due to its ability to carry more weight (sensors and large batteries payload), generate adequate lift (flights at high altitudes) and to maintain stability under the effect of strong turbulent winds when compared to its quadcopter counterpart" [9].

Abarca et al explain that drones experience a decrease in performance at higher altitude, and propeller size, motor, and battery weight were chosen carefully [9]. Stopforth et al. reinforce the notion that an increase in motors means an increase in stability; in addition, more motors will enable heavier payloads [8]. A modular airframe capable of supporting more or fewer motors depending on the conditions would be ideal and reduce fleet size [2]. In short, a drone delivery system should optimize the efficiency through use of MC designs by considering the immediate region and weather and selecting the appropriate amount of motors.

2.1.4 Fixed Wing Designs

Most Fixed Wing (FW) drones are disqualified due to their runway requirements, but any FW capable of VTOL is acceptable. Generally, they have longer flight times than MC's, which made the prospect of a FW VTOL drone alluring. Seeking to combine the best aspects of FW and MC UAV's, Wang et al built and tested a tail-sitter VTOL UAV [10] with flight modes shown in Figure 2.

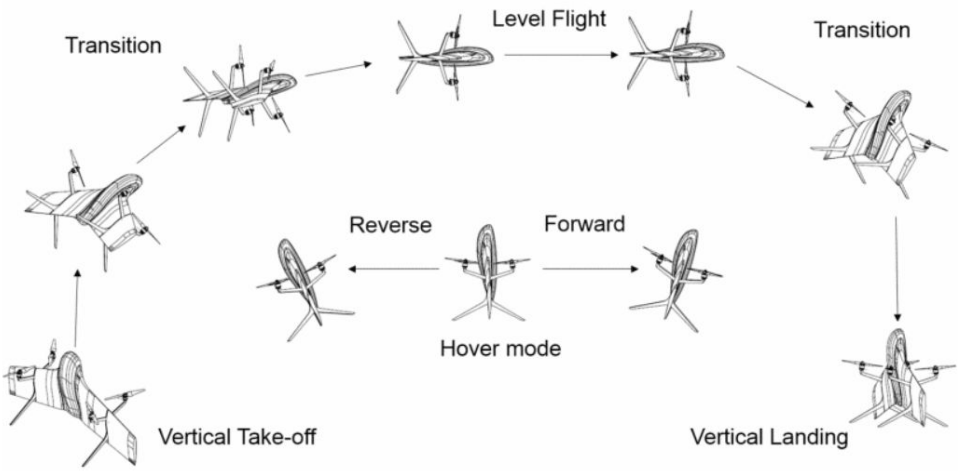

Figure 2: Flight modes of VTOL UAV [10].

The goal was a UAV that incorporated quadcopter VTOL with fixed-wing flight times, utilizing four propellers attached to the wing. The idea itself is nothing new, but the authors had made improvements upon original designs and created new simulation data. They also tested their design against the commercially available DJI Phantom 4, surpassing it in terms of efficiency (flight current), weight, max speed, cross wind resistance, and flight time (Table 2) [10].

Table 2: Phantom 4 vs. tail sitter UAV [10].

Aircraft	Phantom 4	VTOL UAV
Gross Weight	1.45kg	1.35kg
Flight Current	10A	5A
Maximum Flight Velocity	18m/s	25m/s (calculated)
Maximum Flight Time	25mins	40mins (calculated)
Cross Wind resistance	8m/s	5m/s (designed)

Another example of a fixed-wing VTOL drone is the Wingtra, which utilizes only two propellers but boasts a flight time of 60 minutes and a range of 60 kilometers [11], once again demonstrating the tradeoff of propellers for flight time. The Wingtra also accepts payloads, although the weight of 0.5 kg is low compared with MC designs due to its lower propeller count [11].

2.1.5 Deployment Considerations

The drones are to be deployed from trucks, as suggested by Dorling et al. [1], which allows quick adaption of a traditional delivery service to increase last-mile efficiency. As a drone can take around an hour to recharge [2], there will need to be extra batteries onboard the trucks and a way to change them. There should be at least one operator in the truck to drive and load new packages into the drones, but the process of charging and changing the battery can be automated. Liu et al. developed a system named QUADO to handle several batteries and automatically change them into and out of the drone [12]. Finally, the simplest method of separating the package from the drone is to descend and drop the package, but this puts the drone within reach

for easy tampering. A tether system to lower the package from a hovering position at altitude may be a better method, such as Google employs in their delivery drones [5]. Of course, the tether system will add extra weight, and may not offer a discernable difference in time saved from not ascending and descending, but the act of hovering may prove more motor friendly than descending and ascending every time a package is dropped.

2.1.6 Conclusion

Drone delivery has been tested with success and shows promise for bettering any delivery system. Common drone designs have been adapted to deliver, and deploying from trucks allows effective use of available vehicles. Multicopters will likely be the chosen design for any system, and a drone capable of changing configurations (such as between quad- and hexacopter) could reduce necessary fleet size via modularity [2].

There are some aspects that require more research. The tether system's effect on the drone is not fully known. The carrying capacity of FW VTOL's of similar size to multicopters with equal weight and lift generation is assumed to be equal, but lacks absolute proof. Whether it is feasible to expect propellers to be switched as easily as motors is unknown.

2.2 Battery

2.2.1 Charging Schedule

Capacity fading is the degrading of rechargeable batteries due to prolonged charging. By utilizing a charging schedule, costs for battery replacement and charging are kept to a minimum. This requires keeping track of the state of charge (SOC) and state of energy (SOE) of the battery. The SOC indicates the battery capacity as a percentage of total battery life, while the SOE represents the energy available at a specific SOC [15]. [13] describes the typical charging schedule that monitors "the time instances at which a battery begins charging, terminates charging, begins discharging, and terminates discharging." Figure 3 from [13] displays how a charging schedule reduces battery degradation by avoiding overcharge, decreasing the average SOC of the battery and minimizing capacity fading [13].

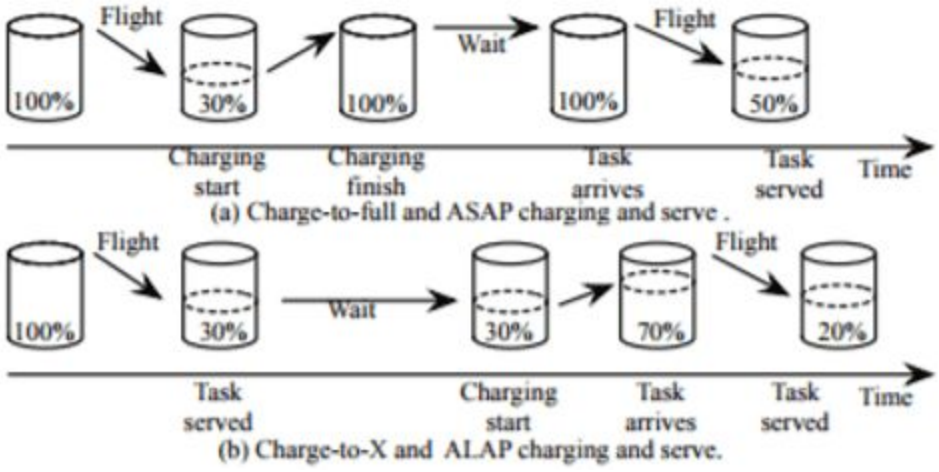

Figure 3: Battery charging schedule [13].

[14] expressed the total cost C_t of drone delivery as:

$$C_t = C_{cp} + C_{op} + C_{udc}$$

C_{cp} represents the total costs for drone and battery components [14]. C_{op} is the cost for system operations, which includes the number of drones and the trips made per day [14]. C_{udc} represents the user cost of waiting for the delivery [14]. Simulations from [14] show that keeping the battery capacity to a minimum will decrease the total cost of delivery by reducing the C_{udc}. C_{cp} and C_{op} will both increase, however this is a result of delivering more packages on average. Therefore, the overall cost will still decrease significantly when using an optimally charged battery. A 10% reduction in total cost is observed when sending delivery drones with 50% battery charge compared to 100% battery charge [14].

2.2.2 Adaptive H Infinity Filter for Charging Schedule

An adaptive H infinity filter will be used to monitor the SOC and SOE of the battery. The filter uses an efficient closed-loop feedback system which allows it to accurately estimate terminal voltages [15]. Covariance matching updates the system's process and measurement noise matrices [15]. Based off these inaccuracy and measured noises, the Kalman gain can be adjusted in real time to minimize the error [15]. The Kalman filter is able to make a more accurate estimation by using a joint probability distribution for variables rather than a single measurement [15]. This makes the closed-loop feedback system more robust against noise disturbances. The

system in [15] utilizes a recursive least square (RLS) method to “identify the battery model parameters in real time”. The RLS is what measures the SOC and SOE of the battery being monitored.

Simulations from [15] show that when the SOC and SOE of a battery were correctly set, the maximum error for SOC and SOE were only 0.04% and 0.06%, respectively. When the initial values for the SOC and SOE were incorrectly set at 80% for a fully charged battery, the adaptive H infinity filter took 35 seconds and 62 seconds, respectively, for the SOC and SOE to converge within an accuracy of 0.1% [15].

2.2.3 Battery Assignment

Delivery drones can use different combinations of Li-ion batteries depending on the distance traveled. Li-ion batteries have a significant impact on the overall weight of the delivery drone. Using the correct combination will lead to a lighter battery, helping improve the flight efficiency. This translates to a smaller energy consumption, helping maintain the state-of-health (SOH) of the battery [13].

Algorithm 1: Battery Assignment Algorithm

Input: S, B
Output: S, B

1: $\{B_k\} = \textbf{groupBatteriesByType}(B)$
2: $\{S_k\} = \textbf{groupBatteriesByEnergy}(S)$
3: **for** $B_k \in \{B_k\}$, $S_k \in \{S_k\}$ **do**
4: $\quad S_k = S_k.\textbf{sortByMetric}(a_i^t - e_i/k^c, min)$
5: $\quad$ **for** $b_j \in B_k$ **do**
6: $\quad\quad b_j.\textbf{appendAttribute}(t_{ea})$
7: $\quad\quad b_j.\textbf{appendAttribute}(S)$
8: $\quad\quad b_j.\textbf{appendAttribute}(order)$
9: $\quad\quad b_j.t_{ea} = 0$
10: $\quad\quad b_j.order = 0$
11: $\quad$ **end for**
12: $\quad$ **while** $false == S_k.\textbf{isEmpty}$ **do**
13: $\quad\quad s_i = S_k.\textbf{popEarliest}()$
14: $\quad\quad b_j = B_k.\textbf{findBatteryByMetric}(t_{ea}, min)$
15: $\quad\quad s_i.b_i = b_j$
16: $\quad\quad b_j.t_{ea} = max(t_{ea} + e_i/k^t + e_i/k^c, a_i^t + e_i/k^t)$
17: $\quad\quad b_j.order = b_j.order + 1$
18: $\quad\quad b_j.S.\textbf{addNewService}([order, s_i])$
19: $\quad$ **end while**
20: $\quad$ **for** $b_j \in B_k$ **do**
21: $\quad\quad b_j.\textbf{deleteAttibute}(t_{ea})$
22: $\quad$ **end for**
23: **end for**
24: **return** S, B

Figure 4: Battery assignment algorithm [13].

Figure 4 displays the battery assignment algorithm proposed by [13]. The first two lines organizes the batteries based on their total capacity and the required energy needed for the task [13]. Line 4 sorts the batteries in ascending order based on the estimated charging time required per flight path [13]. Lines 6-8 "attributes tea, S and order to each battery, which denote respectively the earliest available time of the battery, the services mapped to the battery and the temporal order" [13]. Line 13 orders flight tasks based on their earliest available time, and line 14 estimates which battery will be available first [13]. Lines 15 and 18 then assign the batteries

to their optimal task [13]. This algorithm equips drones with the lightest possible battery that is sufficiently charged for the required flight path.

2.2.4 All Climate Battery for low temperatures

The standard lithium-ion battery performs poorly under cold weather conditions. Attempting to charge a lithium-ion battery at temperatures below freezing will cause permanent capacity loss. Therefore, an external heating component is required to raise the batteries temperature above 0◦C before charging takes place.

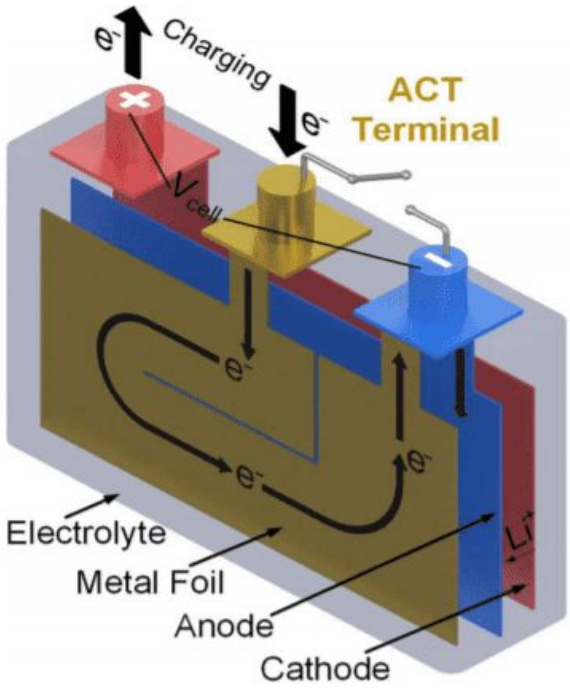

Figure 5: All-climate battery schematic [16].

The all climate battery (ACB) is a lithium-ion battery with an extra component used for heating above 0°C. This extra component is a nickel (Ni) foil with one end connected to the negative

terminal and the other connected to a new terminal called the activation terminal as seen in Figure 5 [16]. A switch is triggered when the battery drops below 0◦C, causing electrons to flow through the Ni foil creating ohmic heat that rapidly warms up the battery [16]. When the battery reaches a temperature above 0◦C, the switch is then turned off and the battery acts as a lithium-ion battery but with high power and low internal resistance [16]. The high power and low internal resistance result from the internal heating which "greatly enhance Li intercalation kinetics in anodes by thermal stimulation of the electrode-electrolyte interface" [17].

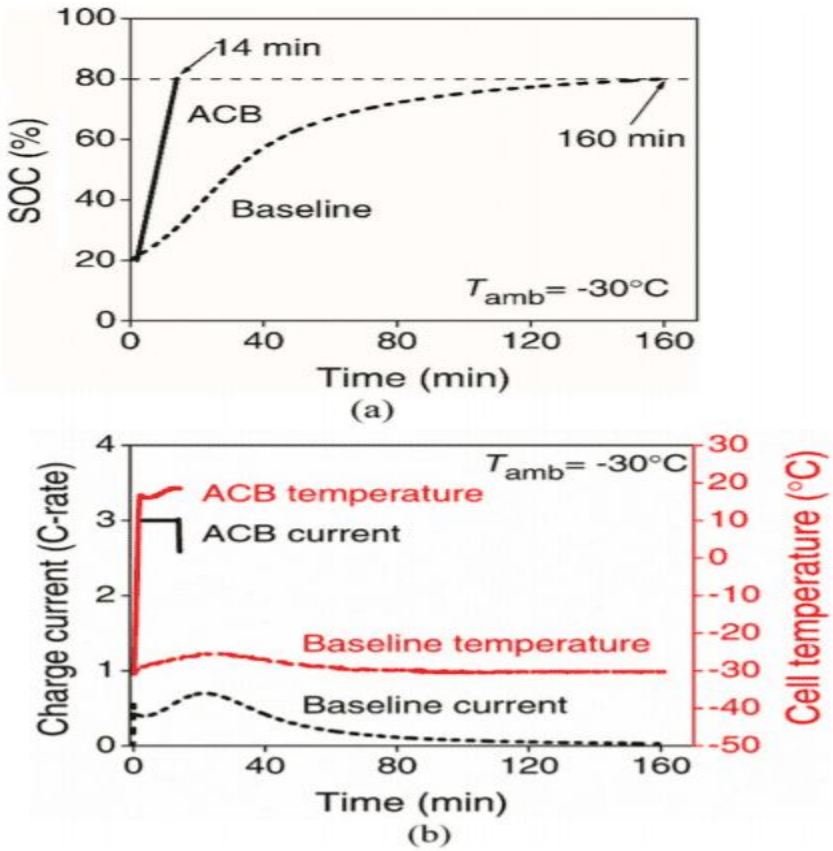

Figure 6: a, SOC versus time. b, charge current versus time [17].

[17] runs simulations that compare the performance of the ACB to a conventional lithium-ion battery. Figures 6a and 6b from [17] show the SOC versus time and charge current versus time for both batteries, respectively. The charge current is expressed in terms of C, which represents the time it takes for a battery to charge or discharge relative to its maximum capacity. For example, a battery charging at 1C will take 1 hour to fully charge, and a battery at 2C with take 30 minutes to charge regardless of the battery's maximum capacity. Both batteries are stored at a temperature of -30◦C and are charged from 20% SOC to 80% SOC. The simulation in [17] does not provide an external heating source for the lithium-ion battery so the temperature stays at -30◦C as seen in Figure 6b. The ACB takes an extra 90 seconds to heat the battery between 10-20◦C to create a "highly reactive electrode-electrolyte interface for high-rate charging" [17]. The total time to charge the ACB is 14 minutes which includes the 90 seconds to raise the battery's core temperature [17]. The lithium-ion battery takes 160 minutes to charge under these conditions, making the charging time 11.4 times faster for the ACB. The ACB is able to keep a charge rate of 2.5-3C while the lithium-ion battery charges at approximately 0.5C and drops to as low as 0.05C [17].

In addition to having a much faster charging time, the ACB is also to maintain its capacity for a longer period of time. The ACB had a loss of 20% total capacity after 500 cycles of charging and discharging, while the traditional lithium-ion battery received the same loss after only 12 cycles [17]. The proposed technology is still currently under development and will still require further testing before it is released for commercial use.

2.2.5 Conclusion

An adaptive H infinity filter will be used to monitor the SOC and SOE for each battery. The SOC and SOE provides information on the optimal battery required for a specific flight path. This will minimize battery degradation and improve delivery time by equipping delivery drones with the lightest battery possible.

The ACB provides an alternative fuel source that performs efficiently in subfreezing temperatures without the need of an external heating source. The ACB is still in the prototype stage but simulations show a decrease in charging time and more resilience to cold climates.

2.3 Routing Algorithm

2.3.1 General Idea of Routing Algorithm

An integrated and developed drone delivery system is not presently available since Amazon's current routing systems focuses on safety and reliability improvements of a single delivery and neglects the ability to process massive delivery orders. [22]. This mathematical routing algorithm attempts to address deficiencies faced by a drone including load limit, flight range and aviation regulations. By coordinating between Unmanned Aerial Vehicles (UAV) and delivery trucks, this routing algorithm optimizes both energy conservation and delivery efficiency [23][24]. The system under this routing algorithm assigns orders to UAV and trucks delivering separately in urban areas, and launches UAV on the truck to expand the flight range in rural and exurban areas [23][24]. Although the real world feasibility and profitability requires further

simulations and investigation, the principles behind the system are mathematically-proved and well-developed.

2.3.2 Flow Network Model

Based on the Mathematical Model "Flow Network," the real-world routing algorithm is converted into an optimization problem with simplified networks shown in the figures below. The entire network consists of two elements, nodes and arcs, where each node represents a customer and each arc directionally connecting two nodes shows the path for delivery vehicles as shown in Figure 7. Green nodes represent customers with UAV capable deliveries while red nodes represent customers with items beyond load limit. The depot point is the starting and ending point of scheduled routes. Dashed arc lines show the UAV's routes while solid lines display the trucks' routes.

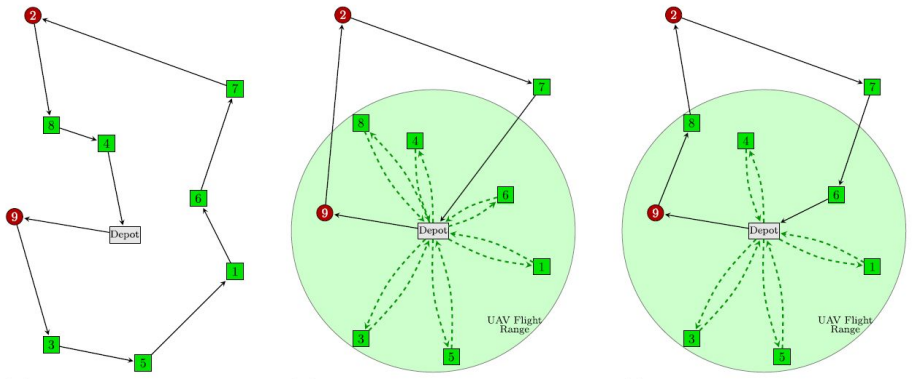

(a) The traditional approach, where a delivery truck visits all customers.

(b) UAVs deliver to all eligible customers within the UAV's flight range; the delivery truck serves customers with large parcels or those outside of flight range.

(c) Optimized assignment of customers to either a UAV or a traditional delivery truck.

Figure 7: Flow Networks for Routing Algorithm in Urban Areas [23].

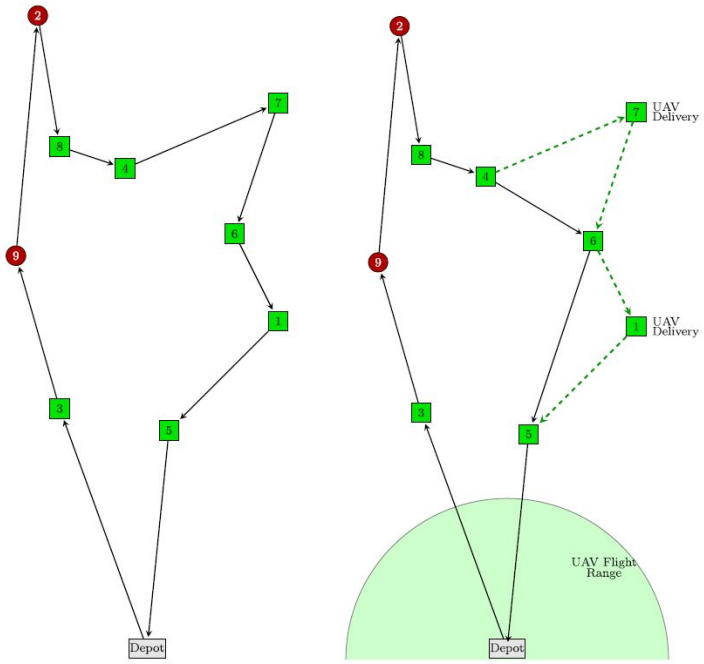

(a) An optimal truck delivery sequence, without the aid of a UAV.

(b) The UAV is launched from a delivery truck, delivering parcels to two eligible customers.

Fig 8: Flow Network for Routing Algorithm in Rural and Exurban Areas [23].

2.3.3 Optimization Problem in Rural and Exurban Areas

In order for the proposed mathematical model to solve the flight route to optimizations, objection function and constraints, need to be applied. Before introducing the specific Mix Integer Linear Programming (MILP) to formulate the problem, there are some parameters, notations and assumptions to be clarified.

Assumptions:

1. This model is motivated by the case that the drone cannot be launched at the depot but coordinated with the truck.

2. Neither drones nor trucks will visit any other points except nodes.
3. Neither drones nor trucks will revisit any delivered nodes.
4. The drone makes one delivery for each sortie, and drone return to truck at another node.
5. While the truck collect the drone at some nodes, the drone will start a new delivery at those nodes.
6. While the drone makes a delivery, truck can make multiple deliveries.
7. Both drones and trucks depart at depot and back to depot.

Parameters and Notations

1. C is the set of customers or delivery addresses. $C = \{1, 2, ..., c\}$, where c equals to number of customers.
2. N is the set of all nodes in the entire network. Nodes 0 denotes the departure point at depot and node c+1 denotes the final return to the depot. $N = \{0, 1, 2, ..., c, c+1\}$
3. N_0 is the set of nodes where vehicles can depart from. $N_0 = \{0, 1, 2, ..., c\}$
4. N_+ is the set of nodes where vehicles can visit. $N_+ = \{1, 2, ..., c, c+1\}$
5. Nodes i refers to starting point. $i \in N_0$
6. Nodes j refers to destination. $j \in N_+$
7. τ_{ij} represents traveling time for trucks from node i to node j
8. τ_{ij}' represents traveling time for drones from node i to node j
9. The form $< i,j >$ stands for path from node i to node j.
10. The form $< i,j,k >$ stands for drone's path launching at node i;delivering at node j and returning at node k. Additionally, all these tuples are included in a set P.

11. The binary decision variable $x_{ij} \in \{0,1\}$ determines whether we choose the path from i to j for trucks.
12. The binary decision variable $y_{ijk} \in \{0,1\}$ determines whether we choose the path launching at i; delivering at j and returning at k for drones.
13. $p_{ij} \in \{0,1\}$ determines whether customer i got delivered before customer j by trucks. Also, we define $p_{0j} = 1$.
14. t_j records the time truck arrives at node j.
15. t_j' records the time drone arrives at node j.
16. u_i records the position of node i in truck's path.
17. s_L is the setup time for launching the drone.
18. s_R is the retrieval time for the drone.
19. M is the a sufficiently large number satisfying $M + \tau_{ij} \to M$ and $M + \tau_{ij}' \to M$.

MILP

Linear Programming is a method to solve the optimization problem in a mathematical model under linear assumption. Generally, linear assumption holds for most of real-world optimization problems including scheduling problems and network problems. Mixed Integer Linear Programming is the linear programming with some of non-integer decision variables.

$$\text{Min} \quad t_{c+1} \tag{1}$$

$$\text{s.t.} \quad \sum_{\substack{i\in N_0\\ i\neq j}} x_{ij} + \sum_{\substack{i\in N_0\\ i\neq j}} \sum_{\substack{k\in N_+\\ \langle i,j,k\rangle\in P}} y_{ijk} = 1 \quad \forall j \in C \tag{2}$$

$$\sum_{j\in N_+} x_{0j} = 1 \tag{3}$$

$$\sum_{i\in N_0} x_{i,c+1} = 1 \tag{4}$$

$$u_i - u_j + 1 \leqslant (c+2)(1-x_{ij}) \quad \forall i \in C, j \in \{N_+ : j \neq i\} \tag{5}$$

$$\sum_{\substack{i\in N_0\\ i\neq j}} x_{ij} = \sum_{\substack{k\in N_+\\ k\neq j}} x_{jk} \quad \forall j \in C \tag{6}$$

$$\sum_{\substack{j\in C\\ j\neq i}} \sum_{\substack{k\in N_+\\ \langle i,j,k\rangle\in P}} y_{ijk} \leqslant 1 \quad \forall i \in N_0 \tag{7}$$

$$\sum_{\substack{i\in N_0\\ i\neq k}} \sum_{\substack{j\in C\\ \langle i,j,k\rangle\in P}} y_{ijk} \leqslant 1 \quad \forall k \in N_+ \tag{8}$$

$$2y_{ijk} \leqslant \sum_{\substack{h\in N_0\\ h\neq i}} x_{hi} + \sum_{\substack{l\in C\\ l\neq k}} x_{lk} \quad \forall i \in C, j \in \{C : j \neq i\}, k \in \{N_+ : \langle i,j,k\rangle \in P\} \tag{9}$$

$$y_{0jk} \leqslant \sum_{\substack{h\in N_0\\ h\neq k}} x_{hk} \quad \forall j \in C, k \in \{N_+ : \langle 0,j,k\rangle \in P\} \tag{10}$$

$$u_k - u_i \geqslant 1 - (c+2)\left(1 - \sum_{\substack{j\in C\\ \langle i,j,k\rangle\in P}} y_{ijk}\right) \quad \forall i \in C, k \in \{N_+ : k \neq i\} \tag{11}$$

$$t'_i \geqslant t_i - M\left(1 - \sum_{\substack{j\in C\\ j\neq i}} \sum_{\substack{k\in N_+\\ \langle i,j,k\rangle\in P}} y_{ijk}\right) \quad \forall i \in C \tag{12}$$

$$t'_i \leqslant t_i + M\left(1 - \sum_{\substack{j\in C\\ j\neq i}} \sum_{\substack{k\in N_+\\ \langle i,j,k\rangle\in P}} y_{ijk}\right) \quad \forall i \in C \tag{13}$$

$$t'_k \geqslant t_k - M\left(1 - \sum_{\substack{i\in N_0\\ i\neq k}} \sum_{\substack{j\in C\\ \langle i,j,k\rangle\in P}} y_{ijk}\right) \quad \forall k \in N_+ \tag{14}$$

$$t'_k \leqslant t_k + M\left(1 - \sum_{\substack{i\in N_0\\ i\neq k}}\sum_{\substack{j\in C\\ \langle i,j,k\rangle\in P}} y_{ijk}\right) \quad \forall k \in N_+ \tag{15}$$

$$t_k \geqslant t_h + \tau_{hk} + s_L\left(\sum_{\substack{l\in C\\ l\neq k}}\sum_{\substack{m\in N_+\\ \langle k,l,m\rangle\in P}} y_{klm}\right) + s_R\left(\sum_{\substack{i\in N_0\\ i\neq k}}\sum_{\substack{j\in C\\ \langle i,j,k\rangle\in P}} y_{ijk}\right) - M(1-x_{hk})$$
$$\forall h \in N_0, k \in \{N_+ : k \neq h\} \tag{16}$$

$$t'_j \geqslant t'_i + \tau'_{ij} - M\left(1 - \sum_{\substack{k\in N_+\\ \langle i,j,k\rangle\in P}} y_{ijk}\right) \quad \forall j \in C', i \in \{N_0 : i \neq j\} \tag{17}$$

$$t'_k \geqslant t'_j + \tau'_{jk} + s_R - M\left(1 - \sum_{\substack{i\in N_0\\ \langle i,j,k\rangle\in P}} y_{ijk}\right) \quad \forall j \in C', k \in \{N_+ : k \neq j\} \tag{18}$$

$$t'_k - (t'_j - \tau'_{ij}) \leqslant e + M(1 - y_{ijk}) \quad \forall k \in N_+, j \in \{C : j \neq k\}, i \in \{N_0 : \langle i,j,k\rangle \in P\} \tag{19}$$

$$u_i - u_j \geqslant 1 - (c+2)p_{ij} \quad \forall i \in C, j \in \{C : j \neq i\} \tag{20}$$

$$u_i - u_j \leqslant -1 + (c+2)(1 - p_{ij}) \quad \forall i \in C, j \in \{C : j \neq i\} \tag{21}$$

$$p_{ij} + p_{ji} = 1 \quad \forall i \in C, j \in \{C : j \neq i\} \tag{22}$$

$$t'_l \geqslant t'_k - M\left(3 - \sum_{\substack{j\in C\\ \langle i,j,k\rangle\in P\\ j\neq l}} y_{ijk} - \sum_{\substack{m\in C\\ m\neq i\\ m\neq k\\ m\neq l}}\sum_{\substack{n\in N_+\\ \langle l,m,n\rangle\in P\\ n\neq i\\ n\neq k}} y_{lmn} - p_{il}\right)$$
$$\forall i \in N_0, k \in \{N_+ : k \neq i\}, l \in \{C : l \neq i, l \neq k\} \tag{23}$$

$$t_0 = 0 \tag{24}$$

$$t'_0 = 0 \tag{25}$$
$$p_{0j} = 1 \quad \forall j \in C \tag{26}$$
$$x_{ij} \in \{0,1\} \quad \forall i \in N_0, j \in \{N_+ : j \neq i\} \tag{27}$$
$$y_{ijk} \in \{0,1\} \quad \forall i \in N_0, j \in \{C : j \neq i\}, k \in \{N_+ : \langle i,j,k\rangle \in P\} \tag{28}$$
$$1 \leqslant u_i \leqslant c+2 \quad \forall i \in N_+ \tag{29}$$
$$t_i \geqslant 0 \quad \forall i \in N \tag{30}$$
$$t'_i \geqslant 0 \quad \forall i \in N \tag{31}$$
$$p_{ij} \in \{0,1\} \quad \forall i \in N_0, j \in \{C : j \neq i\}. \tag{32}$$

[23]

Mathematical Interpretation to MILP

The objective function (1) seeks to minimize the latest time at which either the truck or the UAV return to the depot. Constraint (2) ensures that each customer is visited exactly once. Constraints (3) - (8) regulate vehicles' paths individually. Constraints (3) and (4) ensures that trucks depart

from the depot and return to the depot finally. Constraint (5) is the subtour elimination constraint, and constraints (6) requires the truck to depart from node j after reaching node j. Constraint (7) defines the drone can launch to deliver at all nodes, and constrain (8) defines that drone can return from deliveries at all nodes.

Furthermore, constraints (9) - (26) solve for coordinations between trucks and drones. Constraints (9) - (11) request the truck to visit i before k if the drone launches at i and return at k. In constraints (12) - (15), the drone is forbidden to launch multiple times from the same node and to return at the departure node. Constraint (16) - (19) ensure that scheduling time for vehicles matches. Additionally, constraints (20) - (23) aimed at determining proper values for p_{ij} .

Finally, remaining constraints correspond to both definitions of variables and basic setups.

2.3.4 Optimization Problem in Urban Areas

Similar to the case in rural and exurban areas, majority of setups remain unchanged, and the changes are denoted below.

Assumptions:

1. The model is motivated by the situation that the drone only depart and return at the depot and there is no coordination with the trucks.

Parameters and Notations

1. V is the set of possible nodes visited by the drones.

2. C'' is the set of possible node both within the flight range of the drone and capable for drone delivery.
3. $\widehat{x_{ij}}$ is a new binary decision variable to determine whether we choose the path from i to j for trucks.
4. $\widehat{y_{iv}}$ is a new binary decision variable to determine whether we choose the path from i to v for drones.

MILP

$$\min \quad z \tag{33}$$

$$\text{s.t} \quad z \geq \sum_{i \in N_0} \sum_{j \neq i,\ j \in N_+} \tau_{ij} \cdot \hat{x}_{ij} \tag{34}$$

$$z \geq \sum_{i \in C''} (\tau'_{0i} + \tau'_{i,c+1}) \hat{y}_{iv} \quad \forall v \in V \tag{35}$$

$$\sum_{i \in N_0,\ i \neq j} \hat{x}_{ij} + \sum_{v \in V,\ j \in C''} \hat{y}_{jv} = 1 \quad \forall j \in C \tag{36}$$

$$\sum_{j \in N_+} \hat{x}_{0j} = 1 \tag{37}$$

$$\sum_{i \in N_0} \hat{x}_{i,c+1} = 1 \tag{38}$$

$$\sum_{i \in N_0,\ i \neq j} \hat{x}_{ij} = \sum_{k \in N_+,\ k \neq j} \hat{x}_{jk} \quad \forall j \in C \tag{39}$$

$$\hat{u}_i - \hat{u}_j + 1 \leq (c+2)(1 - \hat{x}_{i,j}) \quad \forall i \in C,\ j \in \{N_+ : j \neq i\} \tag{40}$$

$$1 \leq \hat{u}_i \leq c+2 \quad \forall i \in N_+ \tag{41}$$

$$\hat{x}_{ij} \in \{0,\ 1\} \quad \forall i \in N_0,\ j \in \{N_+ : j \neq i\} \tag{42}$$

$$\hat{y}_{iv} \in \{0,\ 1\} \quad \forall i \in C'',\ v \in V \tag{43}$$

[23]

Mathematical Interpretations on MILP

The objective function (33) seeks to minimize the latest time the vehicles return to the depot. Constraints (34) and (35) defines the lower bound for the latest return time. Constraint (36) guarantees that each customer is visited by exactly one time. Constraint (37) - (39) regulate the routing for trucks to both return to depot eventually and leave the node that a truck enters exactly once. In addition, constraint (40) is the subtour elimination constraint, and constraints (41) - (43) define the decision variables.

2.3.5 Final Solutions

There are two ways to obtain the final solution. Plugging in data provided and inputting decision variables, the MILP solver will calculate the optimization problem and return the optimal solutions. Combining the binary decision variables (xij, yij) with sequencing variable (ui) will present the optimal designs for the delivery routing. Computing optimal solution requires a long time varying from an hour to several days depending on the complexity of the problem, but the optimal solution returned is guaranteed that the objective is optimized by mathematical algorithms.

On the other hand, the heuristic solution is available to provide an estimation of the exact solution. By creating a function to rank possible alternatives offered by a searching algorithm, the heuristic solution is the alternative ranked first under the certain mechanism. Compared to the optimal solution, it always takes less time, but uncertainty and risk exist.

2.3.6 Conclusion

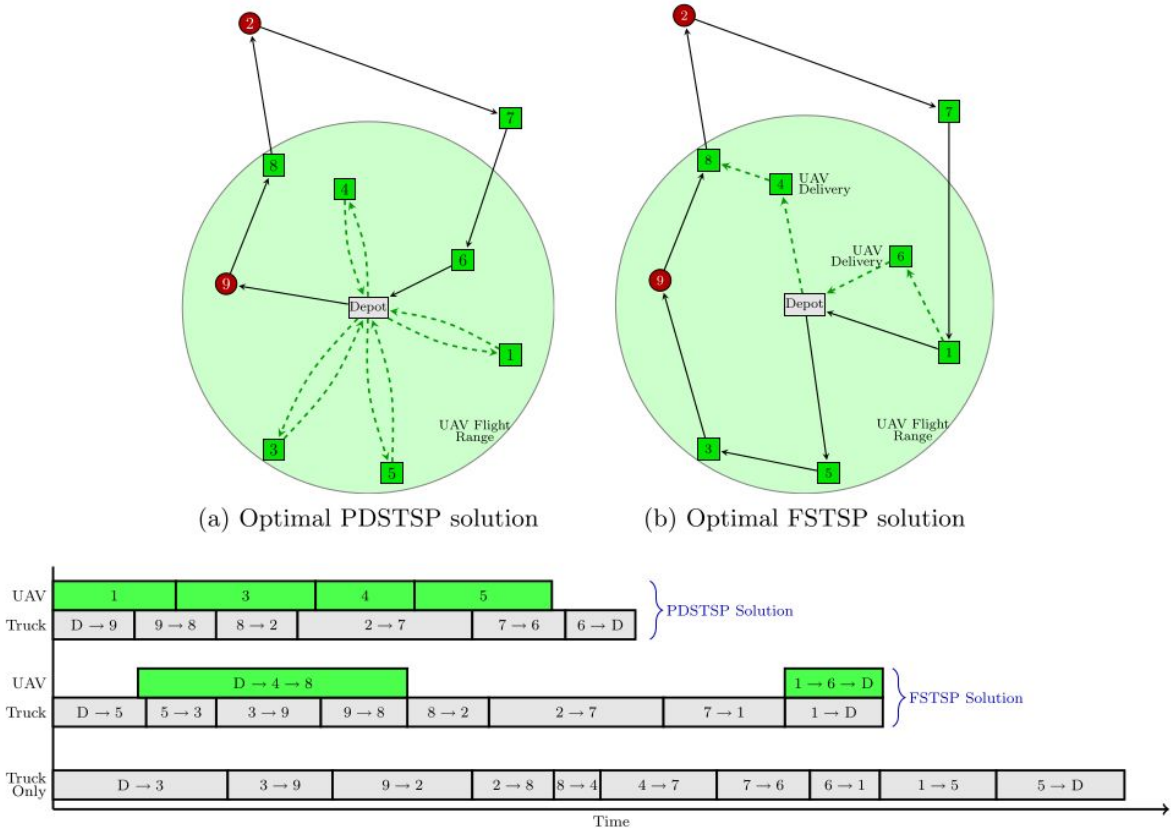

(a) Optimal PDSTSP solution (b) Optimal FSTSP solution

(c) A comparison of delivery schedules for the two systems depicted above. The "Truck Only" schedule represents an optimal TSP solution for a single truck serving all customers.

Figure 9 : Comparison of Optimal Solution between Models [23].

As figure 9 shown, by applying the appropriate model, synchronization and coordination between delivery vehicles shorten the total delivery time by half and reach the customers either outside the drone flight range or with packages beyond load limits.

Improving delivery efficiency by shortening total delivery time; expanding service area restricted by drone flight range; reducing greenhouse gas emission by cutting down the use of petroleum

fuel, the optimization not only develops the advantages of truck delivery but also explore the potential of drone delivery [22][25].

2.4 Cyber Security

2.4.1 Ground Station

A drone's ground station provides a cockpit like interface capable of remote control and communication with the drone. System architecture of professional UAVs include a "telemetry, manual remote control (RC) and video links" [29]. The RC link provides line-of-sight steering functionality within a 100m range using a 2.4 GHz frequency. The telemetry link extends control range to four kilometers while allowing more advanced flight settings through a WiFi enabled flight planning software connection to the XBee 868LP chip on a tablet. An adversary can hijack a drone by successfully connecting to the XBee 868LP chip.

Current ground stations are only capable of providing internal information about the state of the drone based on the telemetry link data (location information and mission state) forcing the user to rely on other sources to determine exterior variables such as weather conditions, wind speeds, magnetic fields, and no fly zones.

2.4.2 XBee 868LP chip

The XBee 868LP chip provides a communication channel through WiFi to an address in memory with a range of four kilometers at a frequency between 863 and 870 MHz [2m]. An XBee chip has a multi-layered firmware structure as shown in Figure 1 that only allows communication between vertically touching interface blocks.The XBee chip stores necessary communication information on an onboard Electronically Erasable Read Only Programmable Memory (EEPROM). The connection parameter information needed to open a communication channel with the XBee chip are the "PAN ID (network ID), BAUD rate, channel, destination high (DH) address and destination low (DL) address" [29]. Although the first three parameters are general knowledge for all UAV's, the remaining two parameters can be obtained from an acknowledgement message received from the XBee chip. Due to the node discovery feature used to connect to nearby XBee chips in Application Programming Interface (API) mode, all received packets are considered valid regardless of the sender's address and receive an acknowledgement packet that exposes all devices on the network by providing the owner's address. The availability of parameter information facilitates man-in-the-middle attacks by hijacking of the drone's communication link through successful connection to the XBee chip. Man-in-the-middle attacks allow adversaries to listen in on the communication between end systems by routing all traffic to them where normal behavior is simulated by forwarding packets between end systems or altering the commands and then forwarding the packets between user and end system.

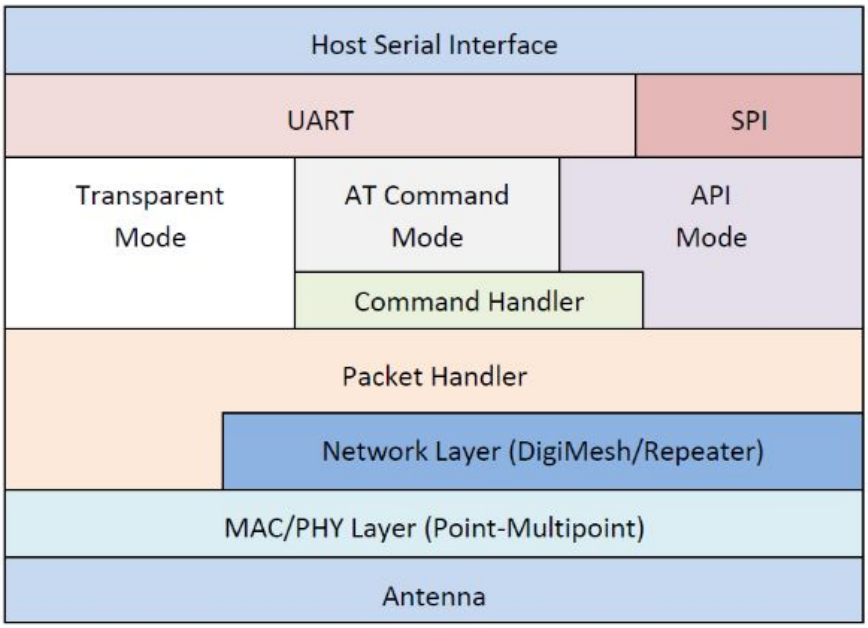

Figure 10: XBee 868LP layered firmware [31].

2.4.3 Remote AT Command

After obtaining all needed parameter information to connect to the XBee chip, a man-in-the-middle attack can be initiated using the "Remote AT command" to reroute traffic and change internal parameters such that it "enables an attacker to understand and alter existing packets in a meaningful way, or inject new packets to communicate with the flight computer" [29]. Transmission of an API frame with new DH or DL parameters is sent to temporarily change the address, followed by the write command in another transmission to permanently change the address used by the XBee chip and since integrity checks are not performed, redirection of all data transfers is possible thus giving the attacker control over the entire system. Figure 11 shows the difference between information routes of a properly operating drone and a compromised drone after a man-in-the-middle attack. Due to the direct connection between the

telemetry link and the software intelligence, exchange is impeded preventing the user from knowing when an attempt to hack the system is being made [30].

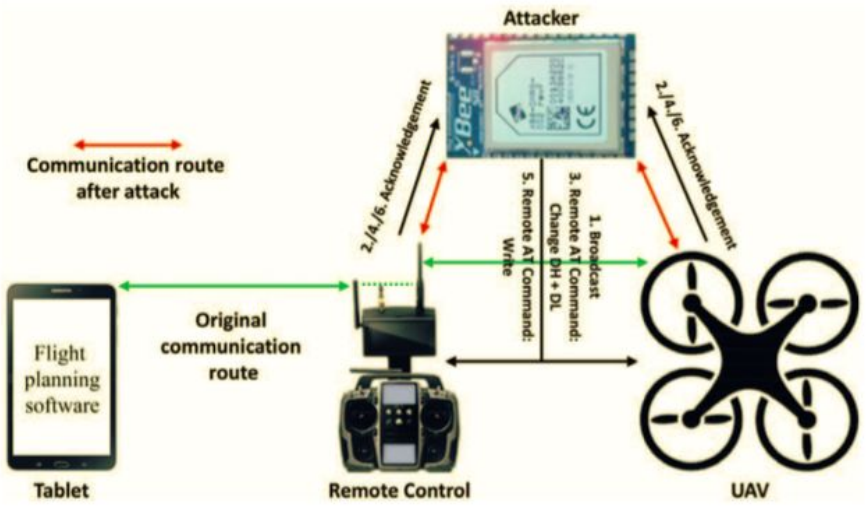

Figure 11: Man-in-the-middle attack [29].

2.4.3 Wi-Fi

Because Wi-Fi uses a crackable encryption scheme, Wired Equivalent Privacy (WEP), an adversary can also hijack a drone's telemetry link by cracking the original user's password to disconnect them, then connecting their own device to it from a physical proximity of 100m. Wi-Fi encryption can be changed to a more secure, less centralized protocol to prevent password cracking and layered with an application layer security protocol like SSL.

2.4.4 Telemetry Link: MAVLink Protocol

The MAVLink protocol provides bidirectional communication between UAV and ground station receivers through a bytewise information transfer following the packet structure in Figure 12.

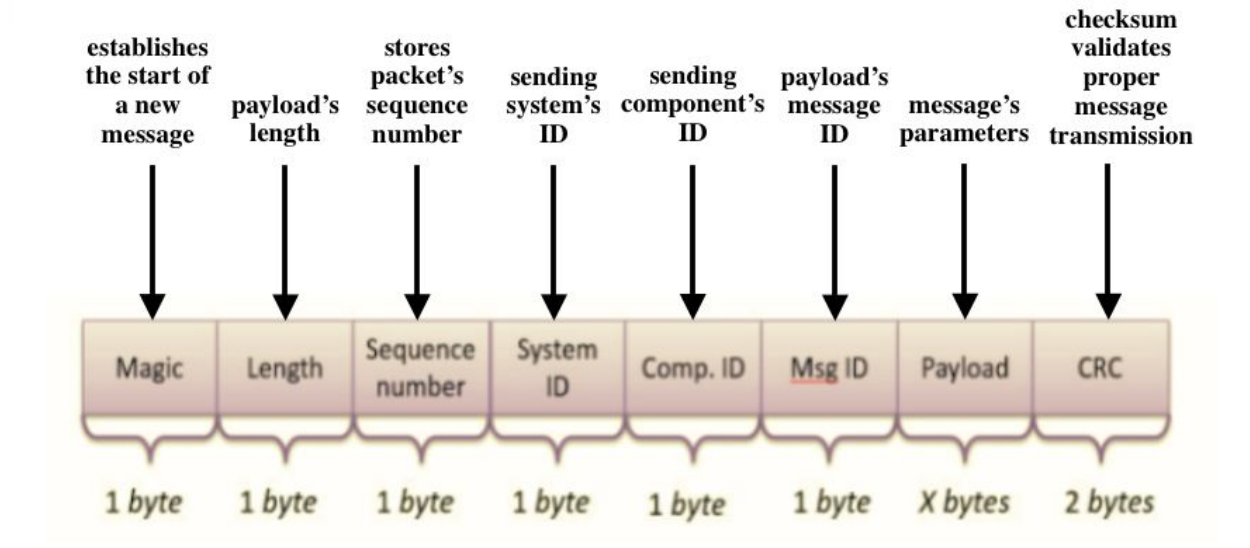

Figure 12: MAVLink message packet structure [32].

The checksum bit is necessary to assure transmission distortion and propagation delay of the network do not corrupt the message. MAVLink uses transmission control protocol (TCP) at its transport layer to allow clear text information to be simultaneously shared by two end hosts without collisions occurring during transmission due to the other's message. TCP is a connection oriented system between two entities which requires an initial three-way handshake of acknowledgement to determine connection parameters before data transfer can be initiated. By current MAVLink implementations only using TCP, a reliable communication connection is provided, not a secure one.

An adversary can crash the end system by fuzzing this protocol. “Fuzzing is a technique for finding vulnerabilities and bugs in software programs and protocols by injecting malformed or semi-malformed data” [28]. Using the structure from Figure 12 for fuzzing, the system can be made to abort its core through injection of packets with random payload lengths until the dedicated memory is exceeded causing the pointer indicating the location of information in memory to point at a non-existent location. The system’s response to abort core is a precautionary action taken to protecting itself; however, this causes the drone to shut down and become a projectile.

Securing MAVLink can be done through the addition of an application layer encryption like Secure Sockets Layer (SSL). SSL is a readily available protocol for existing networks with on-par connection speed between hosts to TCP while providing data integrity through an end-point authentication and encrypted transmission packets instead of clear text.

2.4.5 Microcontroller

A microcontroller is a multipurpose device that acts as a mediator between individual components to create a unified unit which allow for seamless control of its parts. This implementation of the microcontroller allows for communication and customization of an intelligent information exchange link between systems, an onboard software storage, as opposed to the conventional ground station storage, to prevent malfunctions caused by ground station power problems, and an ID unique telemetry module interfaced by radio devices using MAVLink to create a verifiable information connection between radios and the ground station. With the addition of sensors to the drone, a microcontroller can provide a more accurate

information source than reported on outside sources since it will be specific to its current location and state.

2.4.6 Electroencephalogram (EEG) signal

A person's electroencephalogram (EEG) signal is a biometric encryption key system that generates keys every few hours to impede permanent access by an adversary to the device if a key is stolen based on a user's brain activity over a time period T. A battery powered Mindwave EEG sensor "measures and outputs the EEG power spectra (alpha waves, beta waves, etc), NeuroSky eSense meters (attention and meditation), and eye blinks of the user" [27]. This Mindwave sensor stores ground electrodes in an ear clip to provide a reference for measurements made by the headset sensor on the forehead storing EEG electrodes as shown in Figure 13.

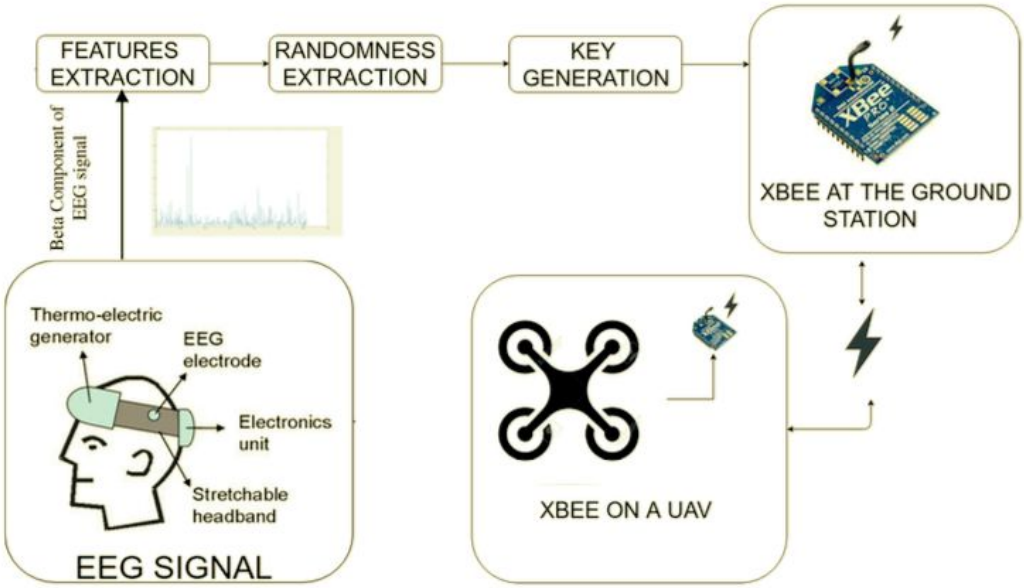

Figure 13: EEG System Configuration [27].

EEG signal analyzes beta waves, which range in a frequency of 12 to 30 Hz, because the subdivision categorization of low beta and high beta allow the extraction algorithm to obtain more specific features from the measured waves. After the information is extracted it is ran through a random linear transformation to prevent an attacker from recreating the signal. Key generation through EEG is unique because successive scans of the same user do not reproduce the same keys guaranteeing a layer of randomness and abstraction.

2.4.7 Encryption

The onboard "XBee's provides the functionality of securing the communication using AES [Advanced Encryption Standard] encryption standard" [27]. The AES algorithm validates and encrypts the data sent to the ground station. In order to verify data has not been tampered with, a Message Authentication Code (MAC) appends a 128-bit key that must match the original key from the user. If an attacker sends a message to the system the mismatching keys will cause a warning flag notifying the system and ground station of a security breach activating an emergency protocol programmed into the microcontroller that takes over the system to block all external communicating connections. The drone then GPS locks its location to prevent GPS spoofing, then send a predefined signal to the ground station to reconfigure link keys and allow it to fly back to safety. By "utilizing brain EEG signal characteristics to generate the cryptographic key for AES data encryption and decryption" of the onboard XBee 686LP chip can close gaps in the telemetry link and remote AT commands [27]. With the addition of encryption to different layers of the system, the remaining outlined cyber security vulnerabilities are addressed. Figure 14 illustrates the communication connections between different parts of a drone network, all

connections through the AES of the XBee chip and user will be using EEG encryption keys while all data flow network connection use SSL to provide a application layer encryption.

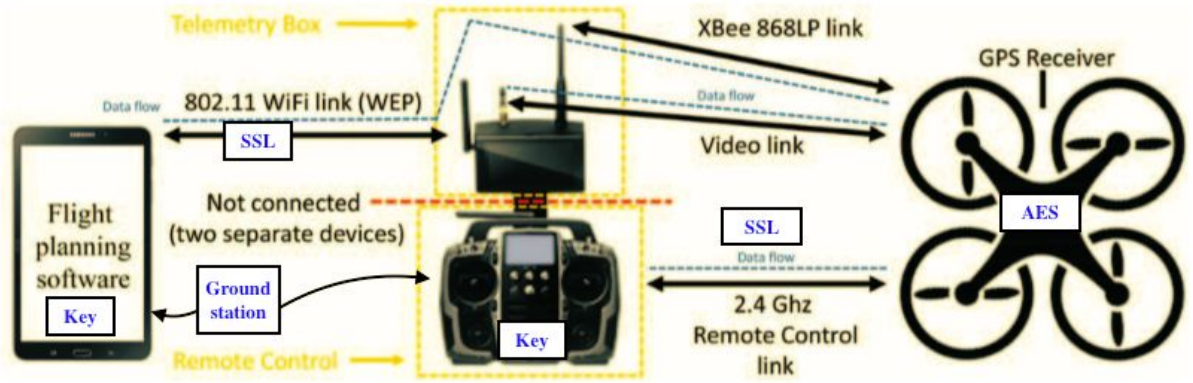

Figure 14: Commercially Available Communication System with Added Features [29].

2.4.8 Conclusion

After these changes are implemented a hacker will be unable to change the path to connect to the drone as shown in Figure 4 because there won't be a backdoor too exploit. With the addition of a microcontroller, EEG signal provides a reliable random key generator that can be used for authentication purposes throughout the network links and prevent intruders from reverse-engineering the signal while providing a more reliable environment information through onboard sensors.

3.0 Criteria and Comparison Strategies

The criteria for the Drone Delivery System are as follows:

- Better routing algorithm improving delivery efficiency
- Cover broader service area
- Reduce battery degradation
- Improved battery efficiency in cold climates
- Drone deployable from truck
- VTOL capabilities, multicopter preferred
- Removable batteries
- Encryption algorithm
- EEG signal for XBee's AES
- Environmental condition data

3.1 Drone Design and Deployment Comparison

Amazon, Google, and UPS are ideal candidates for comparison with a theoretical improved drone delivery system. These entities have been highlighted because they each hold a piece of the puzzle of incorporating drones into a traditional delivery system.

Multicopters are the most chosen platform for aspiring delivery services, with the quadcopter and octocopter being the most represented among major deliverers [33] . Amazon expects to employ multiple types of drones [4], and among those is an octocopter capable of lifting five pounds. UPS also employs an octocopter that is nearly indistinguishable from what Amazon uses [3].

Amazon employs a much larger quadcopter that they deploy from their depots, tested in the UK [4].

Fixed wing craft have received less attention than their iconic cousins, but they have been employed by Amazon and Google. Google avoided traditional MC designs from the start with their Project Wing, initially testing a drone (Figure 15) that bears a striking resemblance to the FW VTOL tailsitter built by Wang et al [10].

Figure 15: Google's initial Project Wing drone, which possesses a five foot wingspan and tether system [5].

However, Google eventually ditched this design, citing control difficulties [5]. Their current design is sort of hybrid between FW and MC platforms, featuring both vertical- and horizontal-facing motors mounted on a fixed wing airframe (Figure 16). Amazon has a similar "Tri-Wing" drone design that they unveiled in 2016 and used to make their first delivery [4].

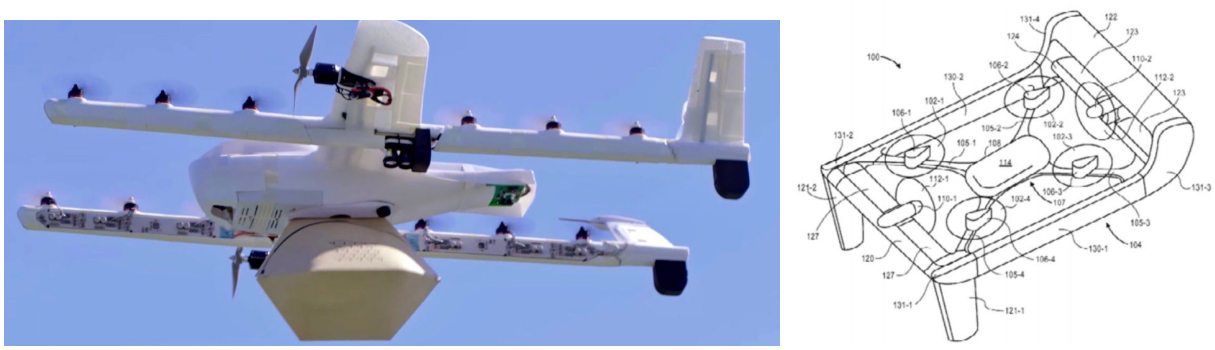

Figure 16 : Google's current FW design [34] vs. Amazon's Tri-Wing [6].

Given the relationship Zulkipli et al. determined between motors and flight time [7], these hybrid designs seem nonoptimal. Google's FW sports an absurd fourteen motors. Amazon's Tri-Wing is much larger than its Google counterpart, currently launched only from warehouses. For each, two of the motors only provide extra weight during ascending and descending. The likes of Amazon and Google may be able to afford nontraditional designs with custom parts, but any smaller entity would be disadvantaged logistically. Being relatively recent designs, weaknesses may not yet be fully explored for these hybrids.

Finally, there's the method of deployment for each company. Google hasn't announced how they will do this yet. Amazon plans to do this from their fulfilment centers, although they have stated plans to position stops on high points such as streetlights and telephone poles [6]. Given Amazon's troubles with the FAA, though, it seems unwise to expect cooperation from public officials. Enough complaints that the installations are ugly attachments to public infrastructure and the plan would fail. Amazon also suggested hitchhiking their drones on delivery trucks when returning to depots [6], but this raises the question of why they do not just employ their own

trucks to carry and retrieve the drones. UPS provides the final piece of the puzzle by using their own modified trucks and drones (Figure 17).

Figure 17: UPS's drone deployment truck [3].

In summary, the need for multiple drone configurations is recognized by Amazon, but they are skirting the deployment question and gambling on extra public support. Google has shown that FW VTOL designs are still not as reliable as the classic MC platforms. UPS has used their trucks in tandem with drones to achieve last-mile efficiency in a manner that would be easy to apply to any traditional delivery system. With modulure MC drones and modified delivery trucks, the ideal drone delivery system can be achieved in a cost-effective manner.

3.2 Battery Comparison

Amazon's current technology for improving battery life includes docking stations for recharging/refueling, a physical metrics acquisition (PMA) device to determine power requirements based on weight distribution, an electricity generation procedure that converts kinetic energy (such as airflow) to generate electricity for battery charging, and a redundant

power generating system that equips drones with a combustion engine to charge the battery or power propellor motors [18-21].

Amazon's currently technology could be improved by implementing the adaptive H infinity filter to monitor the SOC and SOE of their batteries. This would allow them to accurately choose the lightest battery for each specific flight path without requiring all batteries to be fully charged before deployment. Battery degradation would be minimized and flight times will be decreased. The ACB can also be used for drone delivery to improving charging time and increase performance in cold climates.

3.3 Routing Algorithm Comparison

Amazon's routing system concentrated on security and reliability of service within flight range of their drones. Amazon's developing team did not consider to expand their Prime Air service by cooperation with ground shipping companies.

Compared to the Amazon's routing algorithm, our routing algorithm focuses on both synchronization and coordination between delivery vehicles. Under our system, flight range of the drone will be extended by coordinating with the trucks and the drone delivery service will become available for more customers. Without advanced drone's performance and further constructions on depots, our routing algorithm not only expands the service range for drone delivery and but also realizes both the energy conservation and delivery efficiency at the same time.

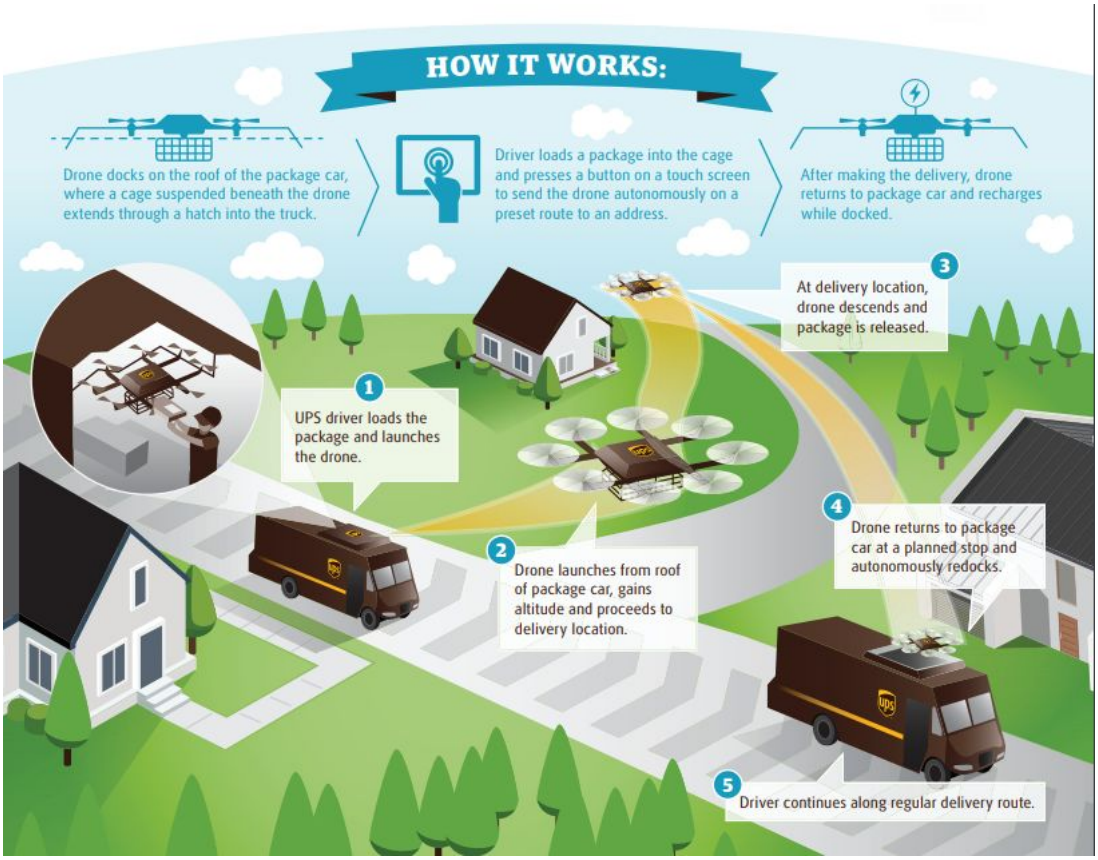

Figure 18 : UPS General Routing Algorithm [26]

3.4 Security Feature Comparison

Security features of current drones being used by Amazon include the ability to detect GPS spoofing and alert the user of the intrusion. When spoofing is detected by the network, control of the device is handed over to another nearby drone or made given a landing procedure. Problems with

3.5 Cyber Security

Amazon's patent describes a mesh network for communication between drones and ground station as show in Figure 19 to expand the reach of control for the systems, however moving UAV "infrastructure towards more network-centric command and control, where all of the components are interconnected through sophisticated mesh networks enables fast communication and constant environmental and asset awareness, but introduces security drawbacks" [27]. With such interconnectivity in a network, compromise of one component can cause failures and malicious behavior to occur throughout the entire network. Although Amazon does take into account the compromise of one system in the mesh, they rely on another drone to be within communication range (four kilometers) to hand over control of the compromised drone to maneuver the drone to safety. They do not however mention GPS locking in their procedure which puts the other drone at risk since GPS spoofing could have made the drone think it was elsewhere cause it to crash with the other system or simple maneuver out of range and crash or be controlled by the adversary. They do address the concern about external condition data though which would help drones maneuver in extreme conditions.

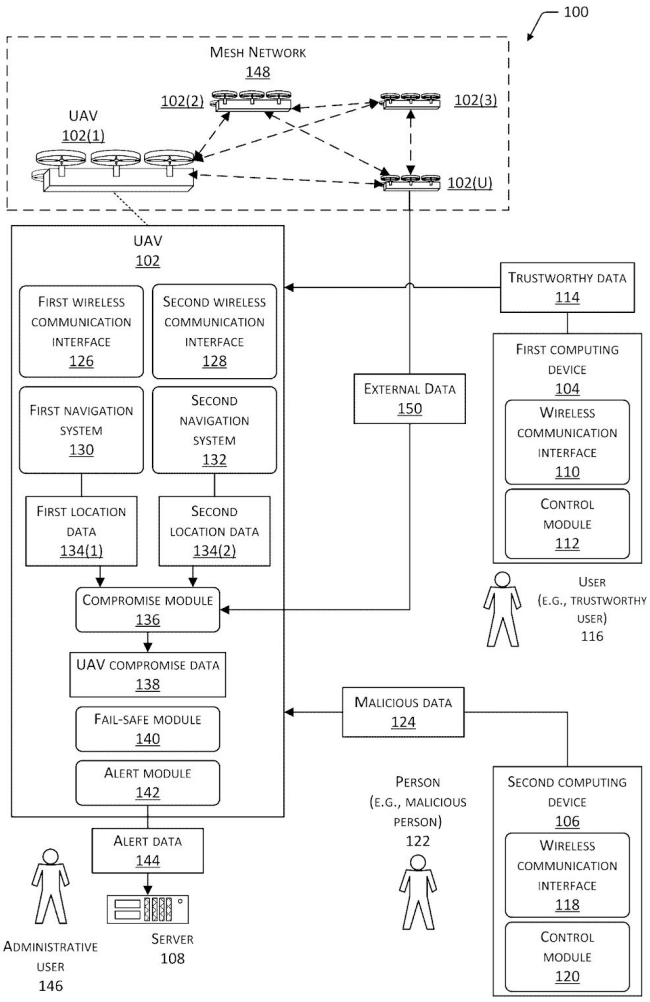

Figure 19: Amazon's Network Architecture [35]

4.0 Recommendation

A modular multicopter design small enough to fit in a delivery truck would be ideal. Modularity would greatly ease the inventory and logistics strain for dealing with a fleet of drones that can operate in many different environments. The batteries need to be removable. For now, a tether system offers little advantage over the drone descending and dropping. Choose the multicopter

configuration with the fewest motors necessary to deal with environmental conditions and payload.

Since service availability is important for customers, our routing algorithm offers a feasible and practical solution to ensure service availability. Furthermore, our routing algorithm reduce the pollution and optimize the delivery efficiency.

We recommend using an adaptive H infinity filter to monitor the SOC and SOE of our delivery drone. This filter has a higher accuracy compared to the widely used KF filter due to its high resilience against noise disturbances. Results from the adaptive H infinity filter will be used to assign drones with the optimal battery per flight path.

Using the ACB over a lithium-ion battery is recommended due to its quicker charging time and high performance in cold climate areas. Even though it is still in the prototype stage, the ACB will reduce the waiting time for deliveries as well as make drone delivery possible in subfreezing regions.

We also recommend using a ground station capable of monitoring outside variables.

5.0 Conclusion

Current drone delivery systems are nonoptimal. Amazon is trying to send all packages directly from its depots and asking to attach charging stations on public utilities. Google has not developed its deployment strategies at all and is experimenting with designs. UPS has one type of drone with no modularity. None of these delivery enterprises have announced a well-developed routing algorithm fulfilling both requirements and expectations from customers.

Amazon currently lacks an efficient way to monitor the drone battery SOC and SOE, preventing them from equipping drones with the lightest battery per flight path. Additionally, no consideration is made for drone delivery in subfreezing regions were an external heating source would be necessary to maintain a functional lithium-ion battery. Current drones lack the ability to provide intelligent information between ground station and UAV, a secure communication channel, and a environmental data.

In our new drone delivery system, modular multicopters are deployed from trucks to effectively handle the last miles. An adaptive H infinity filter will accurately measure the SOC and SOE. The ACB can be used to as an efficient fuel source in subfreezing climates. Our routine algorithm provides better accessibility for customers and makes profit by developing prospective customers. The security vulnerabilities currently exploitable are addressed in this paper through a series of component level encryptions with EEG providing a key generating system that cannot be reverse engineered while providing additional information about environment conditions. We are extremely confident our system is the most efficient method of incorporating drones into delivery operations.

6.0 References

[1] K. Dorling, J. Heinrichs, G. G. Messier and S. Magierowski, "Vehicle Routing Problems for Drone Delivery," in IEEE Transactions on Systems, Man, and Cybernetics: Systems, vol. 47, no. 1, pp. 70-85, Jan. 2017.

[2] J. Lee, "Optimization of a modular drone delivery system," 2017 Annual IEEE International Systems Conference (SysCon), Montreal, QC, 2017, pp. 1-8.

[3] "This UPS Truck Can Deploy an Autonomous Roof-Docked Delivery Drone." Core77, Core77, www.core77.com/posts/69253/This-UPS-Truck-Can-Deploy-an-Autonomous-Roof-Docked-Delivery-Drone.

[4] "Amazon Prime Air." Amazon, Amazon, www.amazon.com/Amazon-Prime-Air/b?node=8037720011.

[5] Phillips, Alan. "Google Scraps Project Wing, Working on New Drone Design." DRONELIFE, Dronelife, 20 Mar. 2015, dronelife.com/2015/03/18/google-scraps-project-wing-working-on-new-drone-design/.

[6] Michel, Arthur Holland. "Amazon's Drone Patents." Center for the Study of the Drone, Bard College, dronecenter.bard.edu/amazon-drone-patents/.

[7] A. Hafifi Zulkipli, T. Raj, F. H. Hashim and A. Baseri Huddin, "Characterization of DC brushless motor for an efficient multicopter design," 2016 International Conference on Advances in Electrical, Electronic and Systems Engineering (ICAEES), Putrajaya, 2016, pp. 586-591.

[8] R. Stopforth, S. Davrajh and A. Ferrein, "Design considerations of the duo fugam dual rotor UAV," 2017 Pattern Recognition Association of South Africa and Robotics and Mechatronics (PRASA-RobMech), Bloemfontein, 2017, pp. 7-13.

[9] M. Abarca, C. Saito, A. Angulo, J. A. Paredes and F. Cuellar, "Design and development of an hexacopter for air quality monitoring at high altitudes," 2017 13th IEEE Conference on Automation Science and Engineering (CASE), Xi'an, 2017, pp. 1457-1462.

[10] Y. Wang, X. Lyu, H. Gu, S. Shen, Z. Li and F. Zhang, "Design, implementation and verification of a quadrotor tail-sitter VTOL UAV," 2017 International Conference on Unmanned Aircraft Systems (ICUAS), Miami, FL, USA, 2017, pp. 462-471.

[11] S. Cass, "Beyond the quadcopter: New designs for drones showcased at CeBIT," 2016, pp. 21-22.

[12] Z. n. Liu, Z. h. Wang, D. Leo, X. Q. Liu and H. w. Zhao, "QUADO: An autonomous recharge system for quadcopter," 2017 IEEE International Conference on Cybernetics and

Intelligent Systems (CIS) and IEEE Conference on Robotics, Automation and Mechatronics (RAM), Ningbo, 2017, pp. 7-12.

[13] Sangyoung Park, Licong Zhang, Samarjit Chakraborty. "Battery Assignment and Scheduling for Drone Delivery Businesses," *Low Power Electronics and Design.* August 2017.

[14] Youngmin Choi, Paul M. Schonfeld. "Optimization of Multi-package Drone Deliveries Considering Battery Capacity," *96th Annual Meeting of the Transportation Research Board.* August 1 2016.

[15] Yongzhi Zhang, Rui Xiong, Hongwen He, Weixiang Shen. "Lithium-Ion Battery Pack State of Charge and State of Energy Estimation Algorithms Using a Hardware-in-the-Loop Validation," *IEEE Transactions on Power Electronics.* Volume 32. June 2017, pp 4421-4431

[16] Chao-Yang Wang, Guangsheng Zhang, Shanhai Ge, Terrence Xu, Yan Ji, Xiao-Guang Yang, Yongjun Leng. "Lithium-ion battery structure that self-heats at low temperatures," *Nature.* Volume 529, January 28 2016, pp 515-518.

[17] Chao-Yang Wang, Terrence Xu, Shanhai Ge, Guangsheng Zhang, Xiao-Guang Yang, Yan Ji. "A Fast Rechargeable Lithium-Ion Battery at Subfreezing Temperatures," *Journal of The Electrochemical Society.* July 13, 2016.

[18] Nicholas Kristofer Gentry. "On-board redundant power system for unmanned aerial vehicles," *Amazon Technologies Inc.* June 28 2016.

[19] Nicholas Kristofer Gentry, Raphael Hsieh, Luan Khai Nguyen. "Multi-use UAV docking station systems and methods," *Amazon Technologies Inc.* December 27, 2016.

[20] Brian C. Beckman, Amir Navot, Daniel Buchmueller, Gur Kimchi, Fabian Hensel, Scott A. Green, Brandon William Porter, Severan Sylvain Jean-Michel Rault. "Electricity generation in automated aerial vehicles," *Amazon Technologies Inc.* January 24, 2017.

[21] Jon T. Hanlon. "Unmanned aerial vehicle physical metrics acquisition," *Amazon Technologies Inc.* May 23, 2017.

[22] Tugrul U. Daim, Leong Chan, Judith Estep. *Innovation, Technology, and Knowledge Management.* Springer International Publishing, 2018, pp.387-412

[23] Chase C. Murray,Amanda G. Chu. *The Flying Sidekick Traveling Salesman Problem: Optimization of Drone-Assisted Parcel Delivery.* Transportation Research Part C: Emerging Technologies Volume 54, May 2015, pp. 86-109

[24] Quang MinhHa, Yves Deville, Quang Dung Pham, Minh HoàngHàc. *On the min-cost Traveling Salesman Problem with Drone.*Transportation Research Part C: Emerging Technologies, Volume 86, January 2018, pp. 597-621

[25] Anne Goodchild, Jordan Toy. *Delivery by drone: An evaluation of unmanned aerial vehicle technology in reducing CO2 emissions in the delivery service Industry.* Transportation Research Part D: Transport and Environment, online, March 2017

[26] UPS Tests Residential Delivery Via Drone Launched From atop Package Car https://pressroom.ups.com/pressroom/ContentDetailsViewer.page?ConceptType=PressReleases&id=1487687844847-162

[27] A. Singandhupe, H. M. La, D. Feil-Seifer, P. Huang, L. Guo, and M. Li (2017). *Securing a UAV Using Individual Characteristics From an EEG Signal*. [online] Arxiv.org. Available at: https://arxiv.org/pdf/1704.04574.pdf [Accessed 6 Feb. 2018].

[28] K. Domin, , E. M. Fàbregas and I. Symeonidis (2016). *Security Analysis of the Drone Communication Protocol: Fuzzing the MAVLink protocol*. [online] www.esat.kuleuven.be. Available at: https://www.esat.kuleuven.be/cosic/publications/article-2667.pdf [Accessed 31 Jan. 2018].

[29] N. M. Rodday, R. d. O. Schmidt and A. Pras, "Exploring security vulnerabilities of unmanned aerial vehicles," *NOMS 2016 - 2016 IEEE/IFIP Network Operations and Management Symposium*, Istanbul, 2016, pp. 993-994.

URL: http://ieeexplore.ieee.org/stamp/stamp.jsp?tp=&arnumber=7502939&isnumber=7502779

[30] S. R. Haque, R. Kormokar and A. U. Zaman, "Drone ground control station with enhanced safety features," *2017 2nd International Conference for Convergence in Technology (I2CT)*, Mumbai, 2017, pp. 1207-1210. URL: http://ieeexplore.ieee.org/stamp/stamp.jsp?tp=&arnumber=8226318&isnumber=8226083

[31] Digi.com. (2018). XBee 868 LP RF Modules User Guide. [online] Available at: https://www.digi.com/resources/documentation/digidocs/pdfs/90002126.pdf [Accessed 7 Mar. 2018].

[32] S. R. Haque, R. Kormokar and A. U. Zaman, "Drone ground control station with enhanced safety features," *2017 2nd International Conference for Convergence in Technology (I2CT)*, Mumbai, 2017, pp. 1207-1210. URL: http://ieeexplore.ieee.org/stamp/stamp.jsp?tp=&arnumber=8226318&isnumber =8226083

[33] "How much weight can delivery drones carry?" UnmannedCargo.org, 23 Oct. 2016, unmannedcargo.org/how-much-weight-can-delivery-drones-carry/.

[34] Kestaloo, Haye. "Alphabet's Project Wing plans to deliver burritos by drone in South Eastern Australia." 9to5Google, 9to5Google, 9to5google.com/2017/10/17/burritos-delivered-by-drone-google-alphabets-project-wing-australia/.

[35] Patents.google.com. (2018). *US9524648B1 - Countermeasures for threats to an uncrewed autonomous vehicle - Google Patents*. [online] Available at: https://patents.google.com/patent/US9524648 [Accessed 9 Mar. 2018].

7.0 Division of Responsibilities:

Erik	Mark	Qixin	Gracie	Everyone
Technical background: drone selection and deployment	Technical background: battery	Technical background: routing algorithm	Technical background: cyber security	Edited and revised entire paper
Comparison: drone design and deployment	Comparison: battery	Comparison: routing algorithm	Comparison: security feature	Wrote transmittal letter, executive summary, abstract, introduction, conclusion, and recommendation sections